Reduced-Order Modeling and Controller Design for a High-Performance Helicopter

Mark Ekblad*
University of Minnesota, Minneapolis, Minnesota 55455

This paper will discuss the use of balanced coordinates for obtaining a reduced-order model and eigenspace assignment techniques for designing a controller for use in precise hover for handling qualities enhancement of a modern attack helicopter. The reduced-order model requires approximately one-third of the number of states of the original model with an additive error norm upper bound of 0.35. Desired transient response characteristics are achieved through eigenvalue assignment and modal decoupling through eigenvector shaping. Loop-transfer recovery techniques are used for the design of a state observer. Stability robustness of the controller is demonstrated using singular-value techniques. Frequency and time responses are used to demonstrate the behavior of the feedback control system. Good closed-loop characteristics are obtained.

Nomenclature

A = open-loop dynamics matrix
B = input distribution matrix
C = measurement distribution matrix, state vector
D = measurement distribution matrix, control vector
E_∞ = additive error norm
G = feedback gain matrix
H = estimator gain matrix
I = identity matrix
i = $\sqrt{-1}$
n_{zcg} = normal acceleration, g
P = prefilter gain matrix
p = roll rate, deg/s
q = pitch rate, deg/s
r = yaw rate, deg/s
u = forward velocity, ft/s
u_c = commanded control vector from prefilter, deg
u_{cr} = directional control vector, deg
u_{cu} = longitudinal control vector, deg
u_{cv} = lateral control vector, deg
u_{cw} = collective commanded control vector, deg
u_p = pilot input command vector, deg
v = lateral velocity, ft/s
W = output distribution matrix for prefilter
w = down velocity, ft/s
x = state vector
y = measurement vector
Δ = multiplicative error measure
λ = eigenvalue
ϕ = roll angle, deg
θ = pitch angle, deg

Functions

$G(s)$ = system transfer matrix $C(sI-A)^{-1}B+D$
$K(s)$ = compensator transfer matrix $G(sI-A+BG+HC)^{-1}H$

Operators

$\|f(s)\|_\infty$ = infinity norm of $f(s)$ = sup$\bar{\sigma}[f(j\omega)]$ over all ω
$\bar{\sigma}$ = maximum singular value
$\underline{\sigma}$ = minimum singular value

Subscripts

coll = collective
dir = directional
lat = lateral
long = longitudinal
r = reduced-order model of rth order
rb = rigid-body dynamics
sa = sensor actuator dynamics
10 = tenth-order system
29 = 29th-order system

Superscripts

H = complex conjugate transpose
T = transpose
-1 = inverse

Introduction

BECAUSE of the extreme coupling between the longitudinal and lateral modes and the open-loop instabilities that exist in most helicopters at hover, manual control of the helicopter at this flight condition is extremely difficult, thus leading to increased pilot work load. These unfavorable characteristics may be substantially improved by using feedback control for modal decoupling and stability augmentation. The objective of this work is to design a suboptimal controller using a reduced-order model to improve handling qualities and decrease pilot work load.

The technique of balanced coordinates is used to obtain a reduced-order model of the helicopter. Reduced-order modeling is motivated by economical and computational reasons. The need for lower-order models and/or controllers is evident in the design of control systems for a large number of aircraft or large space structures where the model is described by an infinite number of first-order differential equations. The control laws for high-order systems are overly complex, thus making implementation difficult. Using a reduced-order model for controller synthesis, one automatically arrives at a reduced-or-

Received Aug. 5, 1988; presented as Paper 88-4501 at the AIAA/AHS/ASEE Aircraft Design, Systems, and Operations Meeting, Atlanta, GA, Sept. 7-9, 1988; revision received Dec. 8, 1988.

*Ph.D. Candidate, Control Science and Dynamical Systems Department; currently, Member of Technical Staff, Rockwell International, Inc. Member AIAA.

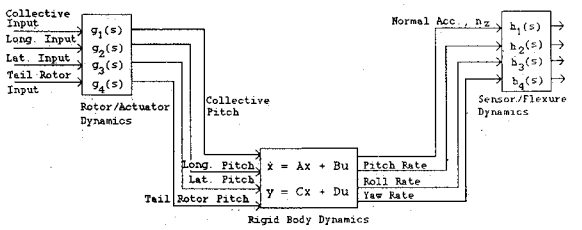

Fig. 1 29th-order model.

Table 1 Transfer functions for rotor/actuator dynamics and flexure/sensor dynamics

$g_1(s) = \dfrac{900}{(30;.46)}$ [a]	$h_1(s) = \dfrac{97.849(12.859)(29.6;.008)}{(31.6;.451)(33.2;.082)}$
$g_2(s) = \dfrac{-40(40)}{(-40)(-40)}$	$h_2(s) = \dfrac{3534.6(12.97;.342)}{(-10.04)(-25.08)(48.6;.036)}$
$g_3(s) = \dfrac{-36.242(80)}{(-80)(-80)}$	$h_3(s) = \dfrac{11.231(-13.209)(120.11)}{(-7.5522)(48.6;.036)}$
$g_4(s) = \dfrac{-20(-56)}{(-20)(-56)}$	$h_4(s) = \dfrac{23.637(-30.841)}{27:.0513}$

[a] (λ) for real eigenvalues, $(\omega_n;\zeta)$ for complex eigenvalues.

der controller. Eigenspace assignment techniques are used to design a stability augmentation system to meet handling qualities requirements and decrease pilot work load. Through spectrum placement, desired time response characteristics and bandwidth can be achieved so that handling qualities requirements are met. To decrease pilot work load, the coupling that occurs between longitudinal, lateral, heave and yaw modes must be alleviated. This is accomplished through eigenvector shaping. A command prefilter is designed to decouple the control input matrix. Loop-transfer recovery techniques are used for the design of the state observer in the feedback loop.

The final control laws must provide for precise control of forward, side, and heave velocity, and yaw rate. This requires that pilot longitudinal stick commands correspond to forward velocity, collective to heave velocity, lateral stick to side velocity, and pedal position to yaw. This is a velocity command system and is intended to provide good handling qualities during precise hover maneuvers. It is also desired that the control laws provide gust attenuation, acceptable stability margins, and meet handling qualities requirements.

The design presented here is only a preliminary step in the process of control system synthesis. Since the model is assumed to be linear throughout, nonlinearities must be accounted for in the final design of the controller and in evaluating its performance. The effect of nonlinearities were not considered for this design.

Mathematical Model

The model used throughout this paper is a 29th-order model typical of a modern high-performance attack helicopter. The model consists of the linearized rigid-body dynamics augmented with actuator and sensor dynamics (see Fig. 1). The transfer functions g_i and h_i, $i = 1,2,3,4$, are given in Table 1. The model is semi-empirical. The linear rigid-body equations were derived from the linearization of the nonlinear equations about the hover trim condition. The input distribution matrix changes significantly when perturbations are taken about the hover trim condition. As stated previously, this fact must be taken into consideration in the latter steps of the design process, but is not treated here. The transfer functions in Fig. 1 were determined from flight test data. The controls for the helicopter consist of main rotor collective pitch, longitudinal cyclic pitch, lateral cyclic pitch, and tail rotor collective pitch. The sensors used in the model are three body-rate gyroscopes and a heave accelerometer. The maximum values that the rigid-body states are expected to achieve during hover flight are as follows: velocities 25 ft/s, angles 20 deg, and angular rates 20 deg/s. The maximum allowable control deflections are as follows: collective 9 deg, longitudinal cyclic 15 deg, lateral cyclic 8.75 deg, and directional tail rotor 18.5 deg.[1] The modes of the open-loop system and the nondimensional rigid-body eigenvectors are given in Tables 2a and 2b, respectively. The nondimensional rigid-body state vector was obtained by dividing the states by their respective maximum values. The nondimensional input control vector was obtained by dividing the four controls by their maximum respective values. The rigid-body states were nondimensionalized to allow for better identification of the modes and their corresponding eigenvectors. The control vector was nondimensionalized to be consistent with the nondimensional state vector.

Examining the open-loop eigenvectors in Table 2b, the cross coupling that occurs between modes is evident. Mode 10 is essentially roll with some yaw coupling. Mode 11 is pitch with

Table 2a Modes of open-loop system

Mode	Eigenvalue	Definition
1	$-1.7448 \pm 48.5687i$	Roll rate flexure/sensor
2	$-1.7496 \pm 48.5685i$	Pitch rate flexure/sensor
3	$-13.8000 \pm 26.6376i$	Collective actuator/rotor
4	$-14.2516 \pm 28.2038i$	Normal accelerometer Flexure/sensor
5	$-2.7240 \pm 33.0881i$	Normal accelerometer Flexure/sensor
6	$-1.3851 \pm 26.9644i$	Yaw rate flexure/sensor
7	-25.0880	Pitch rate flexure/sensor
8	-10.0400	Pitch rate flexure/sensor
9	-7.5522	Roll rate flexure/sensor
10	-3.2610	Roll/helicopter
11	-0.9760	Pitch/helicopter
12	$0.0820 \pm 0.6296i$	Side velocity/helicopter
13	$0.1100 \pm 0.5147i$	Forward velocity/helicopter
14	$-0.2588 \pm 0.0428i$	Heave-yaw/helicopter
15	-56.0000	Directional actuator/tail Rotor
16	-20.0000	Directional actuator/tail Rotor
17	-40.0000	Longitudinal actuator/rotor
18	-36.2420	Lateral actuator/rotor
19	-80.0000	Lateral actuator/rotor

Table 2b Nondimensional eigenvectors of open-loop rigid-body dynamics matrix

	Mode 10	Mode 11	Mode 12	Mode 13	Mode 14
u	-0.0024	0.3605	$-0.0710 + 0.3103i$	$-0.0462 + 0.4723i$	$-0.0244 - 0.1983i$
v	-0.0784	0.0102	$-0.2171 + 0.1269i$	$-0.0979 + 0.1297i$	$0.0616 + 0.0923i$
w	-0.0012	0.0525	$0.0040 + 0.0241i$	$0.0082 + 0.0341i$	$-0.0949 + 0.5468i$
p	-0.8923	0.0373	$0.1334 - 0.2352i$	$-0.0066 - 0.1424i$	$0.0850 + 0.0084i$
q	0.0268	-0.6131	$-0.0234 + 0.2872i$	$0.0666 + 0.2828i$	$0.0488 + 0.0270i$
r	-0.3407	0.3338	$0.3382 + 0.4070i$	$0.4026 + 0.2892i$	$-0.7740 - 0.1489i$
ϕ	0.2844	-0.0767	$-0.2699 - 0.3026i$	$-0.1982 - 0.1093i$	$-0.0231 + 0.0234i$
θ	-0.0030	0.6104	$0.4785 + 0.0727i$	$0.5862 - 0.0431i$	$-0.0257 - 0.0799i$

Table 3 10th-order model and gain matrices

	−0.0286	−0.0637	0.0205	0.2290	7.9700	−0.2570	0.0000	−32.0000	0.0000	0.0000
	0.0779	−0.2310	0.0059	−8.2900	−1.0300	−1.6400	32.0000	0.1640	0.0000	0.0000
	0.0046	−0.0257	−0.2610	−0.3790	2.2500	2.1900	1.6000	−3.2800	0.0000	0.0000
	0.0079	−0.0500	0.0095	−2.7000	−0.1340	−0.6620	0.0000	0.0000	0.0000	0.0000
$A =$	0.0047	0.0118	0.0002	−0.0092	−0.7500	0.0244	0.0000	0.0000	0.0000	0.0000
	0.0039	−0.0049	0.0008	−1.0500	0.4130	−0.4000	0.0000	0.0000	0.0000	0.0000
	0.0000	0.0000	0.0000	1.0000	−0.0051	0.1030	0.0000	0.0000	0.0000	0.0000
	0.0000	0.0000	0.0000	0.0000	0.9990	0.0499	0.0000	0.0000	0.0000	0.0000
	0.0000	0.0000	0.0000	0.0000	0.0000	0.0000	0.0000	0.0000	−2.1869	34.7586
	0.0000	0.0000	0.0000	0.0000	0.0000	0.0000	0.0000	0.0000	−34.7586	−4.5507
	0.4350	0.5760	−0.1140	−0.0009						
	−0.1580	0.1360	0.4910	0.2820						
	−4.2700	0.0575	−0.0250	0.0012						
	−0.0438	−0.0600	0.6470	0.0800						
$B =$	0.0072	−0.1010	−0.0900	−0.0019						
	0.0800	0.0097	0.2000	−0.0455						
	0.0000	0.0000	0.0000	0.0000						
	0.0000	0.0000	0.0000	0.0000						
	1.3276	−0.0109	0.0103	−0.0023						
	1.7491	−0.0255	0.0046	−0.0003						
	0.0000	0.0000	0.0000	1.0000	0.0000	0.0000	0.0000	0.0000	0.0104	0.0008
$C =$	0.0000	0.0000	0.0000	0.0000	1.0000	0.0000	0.0000	0.0000	−0.0021	−0.0010
	0.0000	0.0000	0.0000	0.0000	0.0000	1.0000	0.0000	0.0000	−0.0182	0.0208
	−0.0001	0.0008	0.0081	0.0118	−0.0699	−0.0681	0.0000	0.0000	1.3276	−1.7492
	0.0000	0.0000	0.0000	0.0000						
$D =$	0.0000	0.0000	0.0000	0.0000						
	0.0000	0.0000	0.0000	0.0000						
	0.1327	−0.0018	0.0008	0.0000						
	0.0034	0.0161	−0.0161	0.0820	−0.7626	0.1876	−0.4536	0.4166	0.0000	0.0000
$G =$	0.5345	−0.1732	0.0385	−0.3369	−32.4109	−3.9715	−6.3235	−52.9451	0.0000	0.0000
	0.0625	0.0047	0.0143	0.3257	−0.4237	4.6834	6.8415	−2.6039	0.0000	0.0000
	0.1936	−0.2146	0.0256	21.6137	−21.8732	−45.2356	10.2307	−24.1585	0.0000	0.0000
	−1.5844	241.8895	116.9555	−2.6569						
	−73.8414	54.0384	13.6091	51.8153						
	9.2018	6.8232	7.4105	496.8688						
	10.0985	−0.1241	−0.7049	0.2388						
$H =$	−0.1280	11.5957	0.2590	−0.9404						
	−0.7092	0.2572	11.8640	−0.9402						
	0.0177	0.0536	−0.0914	0.0317						
	0.0178	0.0800	−0.3400	−0.0481						
	0.9760	−0.5505	−2.1368	123.3763						
	0.0644	−0.2759	1.8838	−179.0682						
	0.0772	0.0055	0.0106	0.0124						
$P =$	−0.0524	0.6000	−0.0790	−0.0302						
	−0.0144	0.0300	0.1003	0.1012						
	0.0681	0.2044	0.0311	−0.8352						

inherent forward velocity coupling, which cannot be alleviated. Mode 12 is lateral or side velocity with considerable yaw coupling, some coupling with pitch. Mode 13 is forward velocity with extensive yaw coupling, some coupling with roll, side velocity, and inherent coupling with pitch. Mode 14 is essentially a coupled heave-yaw mode. In examining the input distribution matrix in Table 3, one can see the considerable coupling and the influence the control inputs have on forward, side, and heave acceleration. Main rotor collective pitch and longitudinal cyclic pitch have approximately the same effect on forward acceleration. Lateral cyclic pitch has primary effect on side acceleration with some tail rotor collective pitch contribution. Heave acceleration is chiefly effected by main rotor collective pitch. Roll and pitch accelerations are effected primarily by lateral cyclic and longitudinal cyclic, respectively. Finally, yaw acceleration is influenced significantly by lateral cyclic pitch. This control coupling requires the design of a prefilter to convert pilot inputs to control inputs to achieve the desired type of closed-loop responses.

The preceding description indicates that this model is an excellent candidate for reduction of order and eigenstructure assignment. A similar model was validated by the design of a different type of flight control system and its successful flight test.[2]

Reduced-Order Model

The objective of a reduced-order realization is that the states of the reduced model approximate the behavior of the states of the true model, and that the outputs of the reduced-order model match the output response of the true system. The problem can be formulated in the following manner: consider the system given by

$$\dot{x} = Ax + Bu \tag{1a}$$

$$y = Cx + Du \tag{1b}$$

where the dimension of the state vector x is n, the input vector u has dimension m, and the output vector y has dimension p. The order-reduction problem is to use some technique such as truncation, residualization, balanced coordinates, etc., to find a reduced-order model of dimension r ($r \ll n$) that approximates the true model with respect to some desired measure. The measure of "goodness" of the reduced-order model may

be some error criteria in the frequency and/or time domain and is highly dependent on the purpose for the reduced-order model and the particular application.

Balanced coordinates or balanced singular values is the technique used for reduction of the helicopter model.

The technique of balanced singular values is similar to the concept of principal coordinates and the modal matrix. For balanced singular values, a coordinate system is found such that in that coordinate system the observability and controllability grammians are equal and diagonal. Consider the system described by Eq. (1). The controllability grammian U and observability grammian Y are

$$U = \int_0^\infty e^{At} B B^T e^{A^T t}\, dt \tag{2}$$

$$Y = \int_0^\infty e^{A^T t} C^T C e^{At}\, dt \tag{3}$$

The grammians can be calculated from the Lyapunov equations:

$$AU + UA^T + BB^T = 0 \tag{4a}$$

$$YA + A^T Y + C^T C = 0 \tag{4b}$$

When a system's controllability and observability grammians are equal, the system is defined by Moore[3] to be internally balanced. In this balanced coordinate system the system's grammians are given by

$$U = Y = \Sigma = \text{diag}(\sigma_1, \sigma_2, \ldots, \sigma_n)$$

$\sigma_1 \geq \sigma_2 \geq, \ldots, \geq \sigma_n > 0$ (≥ 0 if original system is not minimal)

where σ_i are the singular values of the system or second modes. The transformation to balanced coordinates can be computed with different techniques. The most computationally efficient and numerically accurate is a technique developed by Laub.[4] This is the technique used here.

Once the system is transformed into a minimal internally balanced realization, a reduced model of rth order, where $\sigma_r \gg \sigma_{r+1}$ is obtained by truncating $n-r$ states of the balanced matrices. This will yield an internally balanced dominant subsystem. An internally balanced realization is the essentially unique realization of an asymptotically stable transfer function that has the following important property: the direction of a given basis vector for the state-space representation is as controllable as it is observable. The lengths of the vectors of the controllability (or observability) grammian provide a scalar measure (singular values) of how controllable *and* observable a given basis vector is. Since this is the case, the dominant subsystem will be a good approximation of the true model since it rejects the least controllable and observable states of the system.

Since the system must be asymptotically stable to find an internally balanced realization, and this model is not, the system must be decomposed into a stable and unstable part, i.e.,

$$G_{\text{true}}(s) = G_{\text{stable}}(s) + G_{\text{unstable}}(s) \tag{5}$$

then the stable part is balanced, and the reduced-order model is obtained by augmenting the unstable system with the desired balanced states. This particular decomposition is not compatible with eigenstructure assignment since six of the eight rigid-body states would lose their physical interpretation due to the transformation to balanced coordinates,[5] thus hampering the intuitive choice of mode shapes.

It is proposed to decompose the system into the following:

$$G_{\text{true}}(s) = G_{sa}(s) + G_{rb}(s) \tag{6}$$

where $G_{sa}(s)$ is the matrix transfer function for the sensor and actuator dynamics. This decomposition was achieved by transforming the system into Jordan coordinates, reordering the states, and transforming the rigid-body states to their original form to arrive at

$$\begin{bmatrix} \dot{x}_{rb} \\ \dot{x}_{sa} \end{bmatrix} = \begin{bmatrix} A_{rb} & 0 \\ 0 & A_{sa} \end{bmatrix} \begin{bmatrix} x_{rb} \\ x_{sa} \end{bmatrix} + \begin{bmatrix} B_{rb} \\ B_{sa} \end{bmatrix} u \tag{7a}$$

$$y = [C_{rb} \quad C_{sa}] \begin{bmatrix} x_{rb} \\ x_{sa} \end{bmatrix} + D_{rb} u \tag{7b}$$

Laub's algorithm[4] was applied to the sensor-actuator realization. The singular values for the balanced system are

(0.4031, 0.3362, 0.1051, 0.0902, 0.0549, 0.0432, 0.0406,

0.0377, 0.0352, 0.0315, 0.0176, 0.0138, 0.0122, 0.0096,

0.0021, 0.0013, 0.0009, 0.0005, 0.0002, 0.00006, 0.00001)

The following models are proposed:

1) 8th order: rigid-body states

2) 10th order: rigid body augmented with two balanced states

3) 12th order: rigid body augmented with four balanced states

4) 18th order: rigid body augmented with ten balanced states

Model 1 is an obvious starting point; however, it does not take into account any of the higher-order modes, which may cause problems with regard to stability robustness. Model 2 is the rigid-body dynamics augmented with poles at $-3.3688 \pm 34.7385i$. Model 3 is the rigid-body dynamics augmented with poles at $-3.0019 \pm 34.554i$ and $-2.3879 \pm 26.1707i$. Model 4 consists of the rigid-body states augmented with poles at $-1.7469 \pm 48.3708i$, -3.0496 ± 34.3204, -2.6995 ± 26.5589, -1.6451 ± 27.2124, -9.1149, and -2.7934. To determine which model is "best," two measures were used. The first is an additive error norm defined by

$$E_\infty = \| G_{\text{true}}(s) - G_r(s) \|_\infty \tag{8}$$

where $G_r(s)$ is the transfer-function matrix of the reduced-order model. This measure yields a maximum relative error bound. The second measure is a multiplicative error defined by

$$\Delta(s) = I - G_r^{-1}(s) G_{\text{true}}(s) \tag{9}$$

This measure gives a nondimensional error that parameterizes the error due to unmodeled dynamics and is the error measure used in the stability robustness theorem.[6] The E_∞ errors for models 1-4 are 1.0368, 0.3537, 0.235, and 0.247, respectively. The maximum singular value of the multiplicative error is shown in Fig. 2. Examining the peak of $\bar{\sigma}[\Delta(s)]$ from Fig. 2, model 3 has a magnitude of 41.125, model 1 34.88, model 2 34.75, and model 4 has the smallest value of 11.4866. From these two measures alone it appears that model 4, the 18th-order model, approximates the true model the best. This fact makes intuitive sense; the more structure the model has the better the approximation. However, this is not always the case and cannot be implicitly assumed. But the purpose of the reduced-order model is to find the minimum-order model that best approximates the true system. Thus, model 4 was eliminated due to its high order. Because model 3 has the largest multiplicative error, it can also be discarded. This leaves models 1 and 2. Model 2 was chosen because it has more structure and smaller E_∞ and multiplicative error. The dimensional state-space matrices for the 10th-order model are given in Table 3.

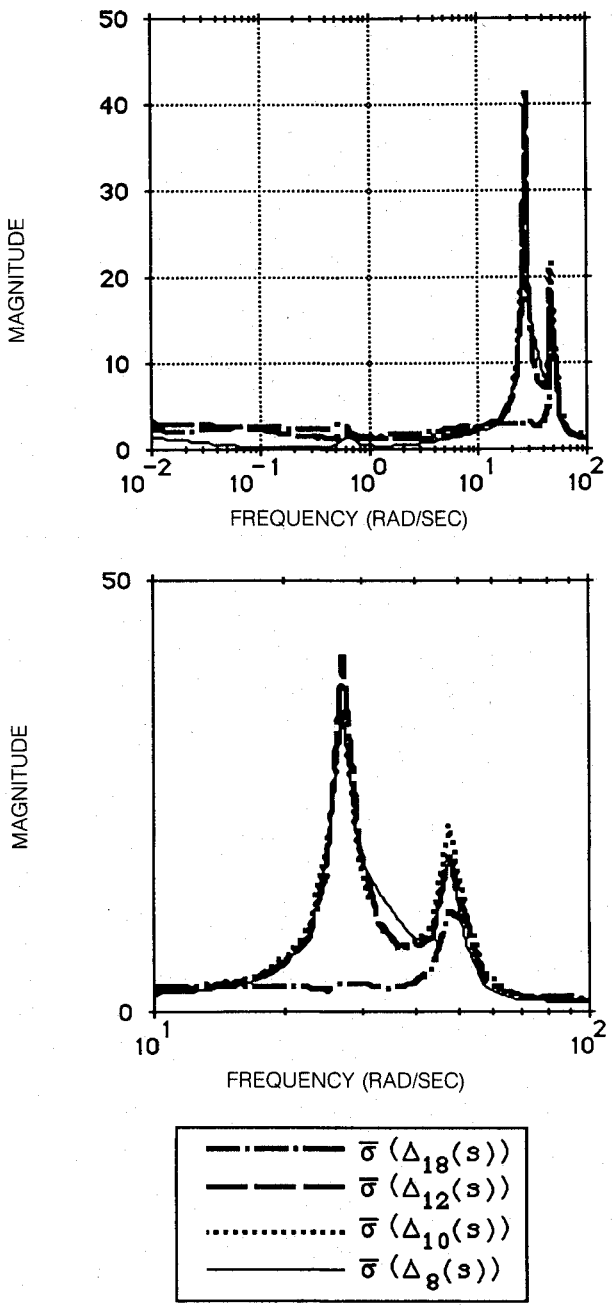

Fig. 2 Maximum singular value of multiplicative error.

Controller Design

The technique of eigenstructure assignment together with loop-transfer recovery will be used to design a controller that meets handling qualities requirements and decreases pilot work load. Using the benefits of eigenstructure assignment, one can choose response times or specify bandwidth, but more importantly, the designer is able to perform modal shaping with eigenvectors (for details of eigenstructure assignment see Refs. 7 and 8). The choice of eigenvalue/eigenvector pairs is dependent upon the particular responses and desired mode shapes. For an attack helicopter, first-order responses in pitch, roll, heave, and yaw are desirable.[9] For level 1 handling qualities, a minimum bandwidth of 2 rad/s is required. In first-order systems, bandwidth and eigenvalues are synonymous. Desirable time constants for yaw, pitch, and roll fall into the range of 0.3 to 0.375 s, which corresponds to eigenvalues ranging from 2.67 to 3.3 rad/s. The heave time constant is approximately 3 s (depending on the usable cue environment[9]) for a desirable response, which implies an eigenvalue of 0.33 rad/s. Second-order responses are desirable for forward and lateral velocity and also require a minimum of 2 rad/s bandwidth to meet level 1 handling qualities requirements. Mitchell and Hoh[9] relate bandwidth, damping factor, and natural frequency by the following equation:

$$\omega_{bw} = \omega_n\left(\zeta + \sqrt{1+\zeta^2}\right) \tag{10}$$

where ω_{bw} is bandwidth, ω_n is natural frequency, and ζ is the damping factor. Equation (10) holds for $\zeta > 0.3$ and no delays present. As stated previously, the system is highly coupled, and it is desirable to decouple the system through modal shaping. Coupling between heave, yaw, longitudinal, and lateral modes should be minimized to decrease pilot work load. Although total decoupling cannot be achieved due to the inherent relationship between some modes, significant improvement can be made to enhance handling qualities.

In the assignment of eigenvalues/eigenvectors, the balanced states were left unchanged. Since they satisfied the minimum bandwidth requirement and were decoupled open loop, there is no reason to change them. Mode 14, coupled heave-yaw, was decoupled into two first-order modes. The heave mode was assigned an eigenvalue of -0.33 and an eigenvector as seen in Table 4. The yaw mode was assigned an eigenvalue of -3.3 and a mode shape decoupled from heave and the remaining states. Mode 11, pitch, was assigned an eigenvalue of $\lambda = -2.8$ to satisfy the previously mentioned constraints. In the case of the pitch mode shape, it is coupled with forward velocity. For forward velocity, an arbitrary value was assigned to the corresponding eigenvector state, but for the case of pitch it was assigned the value of $1/\lambda$ and pitch rate the value of

Table 4 Desired eigenvalues/eigenvectors for 10th-order system

Roll	Pitch	Side	Forward	Heave	Yaw	Balanced
0.0000	−0.1500	0.0000	1.0000	0.0000	0.0000	0.0000
0.1500	0.0000	1.0000	0.0000	0.0000	0.0000	0.0000
0.0000	0.0000	0.0000	0.0000	1.0000	0.0000	0.0000
1.0000	0.0000	0.1000	0.0000	0.0000	0.0000	0.0000
0.0000	1.0000	0.0000	0.3000	0.0000	0.0000	0.0000
0.0000	0.0000	0.0000	0.0000	0.0000	1.0000	0.0000
−0.3067	0.0000	0.2000	0.0000	0.0000	0.0000	0.0000
0.0000	−0.3600	0.0000	0.3000	0.0000	0.0000	0.0000
0.0000	0.0000	0.0000	0.0000	0.0000	0.0000	$0.7067 \pm 0.0240i$
0.0000	0.0000	0.0000	0.0000	0.0000	0.0000	$0.0000 \pm 0.7071i$

Roll: $\lambda = -3.2610$
Pitch: $\lambda = -2.8000$
Side velocity: $\lambda = -0.8057 \pm 0.2681i$
Forward velocity: $\lambda = -0.8157 \pm 0.2681i$
Heave velocity: $\lambda = -0.3300$
Yaw: $\lambda = 3.3000$
Balanced states: $\lambda = -3.3688 \pm 34.7385i$

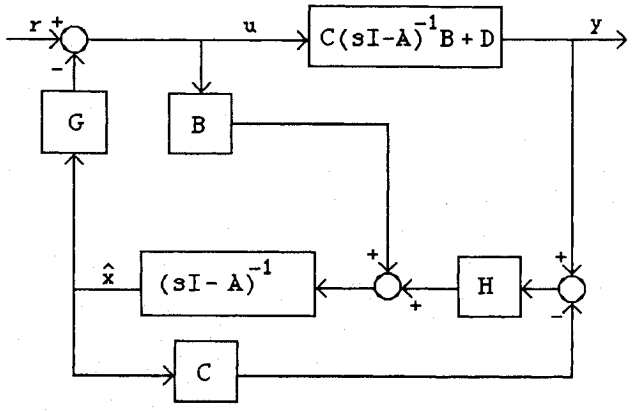

Fig. 3 Combined regulator/estimator.

unity because in the translational equations $q = \theta * \lambda$. The roll modes eigenvalue is left unchanged since it satisfies handling qualities requirements. The eigenvector was assigned in the same manner as pitch. An arbitrary value was assigned in the lateral velocity state, and $1/\lambda$ was assigned to the state corresponding to roll and unity to roll rate. Mode 12, lateral velocity, is unstable and, therefore, must be stabilized. The desired eigenvalue was chosen as $\lambda = -0.8057 \pm 0.2681i$. This implies that $\omega_n = 0.85$ rad/s, $\zeta = 0.95$, and $\omega_{bw} = 2$ rad/s.

The mode shape cannot be totally decoupled. As seen in its eigenvector, lateral velocity is directly related to roll and roll rate. Small arbitrary values were assigned to roll and roll rate and unity to the lateral velocity component. Similarly, mode 13 is also unstable and must be stabilized. Using the same properties as in mode 12, the desired eigenvalue was perturbed slightly to make the mode distinct, which resulted in $\lambda = -0.8157 \pm 0.2681i$. The relationship between pitch and forward velocity again forces one to place small arbitrary values in the mode shape in the states corresponding to pitch and pitch rate.

Once the eigenvalue/eigenvector pairs are decided upon, the feedback gain required to achieve them is calculated by a technique described in Ref. 7. To achieve the desired eigenvectors, they must lie in the range of the column space of $(\lambda I - A)^{-1}B$. This is not always possible. The algorithm used allows one to minimize the mean square error between the desired and attainable eigenvectors. Since there exists some freedom in the choice of the eigenvalues, an iteration procedure was used for each mode to determine the eigenvalue that yielded the smallest error, in a least-squares sense, between the desired and attainable eigenvectors. The eigenvalues ranged over a bandwidth of 2 rad/s. The minimum bandwidth of 2 rad/s was required by level 1 handling qualities requirements. The maximum bandwidth of 4 rad/s was the limiting factor to account for model uncertainty to obtain acceptable stability margins. The author believes that one can find a theoretical relationship for this "optimum" eigenvalue that minimizes the distance between the desired eigenspace and the allowable eigenspace. The dimensional feedback gain G obtained is given in Table 3.

Since the full state regulator requires knowledge of all the states, and this is not always possible, an estimator must be designed to make the compensator realizable. The estimator is given by

$$u = -G\hat{x} \tag{11a}$$

$$\dot{\hat{x}} = A\hat{x} + Bu + H(y - C\hat{x} - Du) \tag{11b}$$

The block diagram of the combined regulator/estimator is shown in Fig. 3. For recovery, the estimator gain H is chosen such that $A - HC$ is stable, and the performance of the combined regulator/estimator matches that of full state feedback design. The estimator gain H was determined using the loop-transfer recovery (LTR) technique described in Ref. 10. The technique involves varying the control weight in the linear-quadratic performance index

$$J = \int_0^\infty (x^T Q x + \rho u^T u) \tag{12}$$

until the singular values of $K(s)G(s)$ approach those of $G(sI - A)^{-1}B$. As ρ approaches 0, LTR is achieved. Figure 4 shows the maximum singular value of $G(sI - A)^{-1}B$ and $K(s)G_r(s)$.

Full recovery was not possible since the 10th-order model is nonminimum phase. Better recovery can be obtained than is demonstrated in Fig. 4, but this results in excessively high gains that may cause problems in implementation. The dimensional estimator gain H for $\rho = 1 \times 10^{-4}$ and $Q = BB^T$ is given in Table 3.

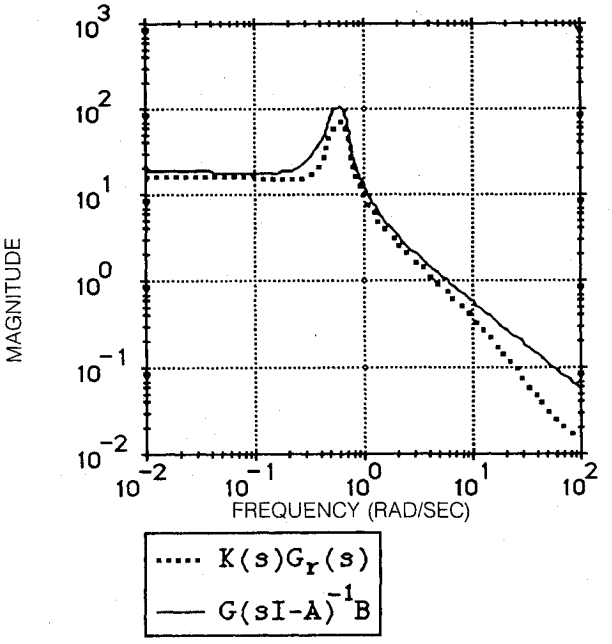

Fig. 4 Maximum singular values of loop-gain function and $G(sI - A)^{-1}B$.

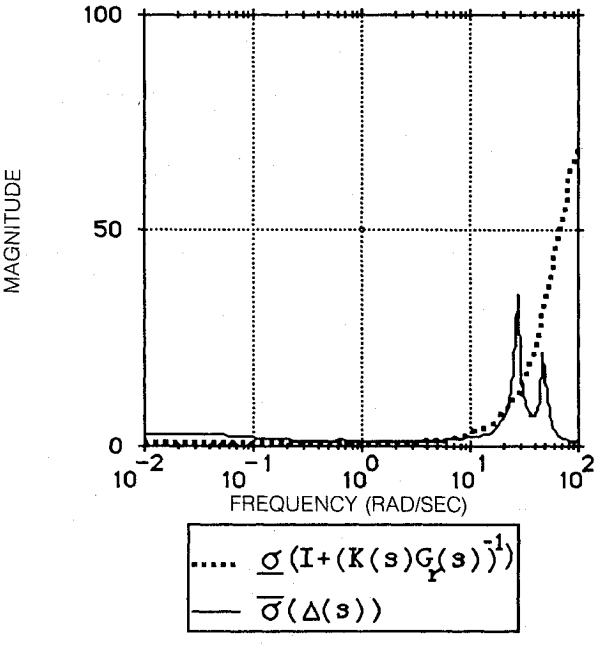

Fig. 5 Stability robustness test.

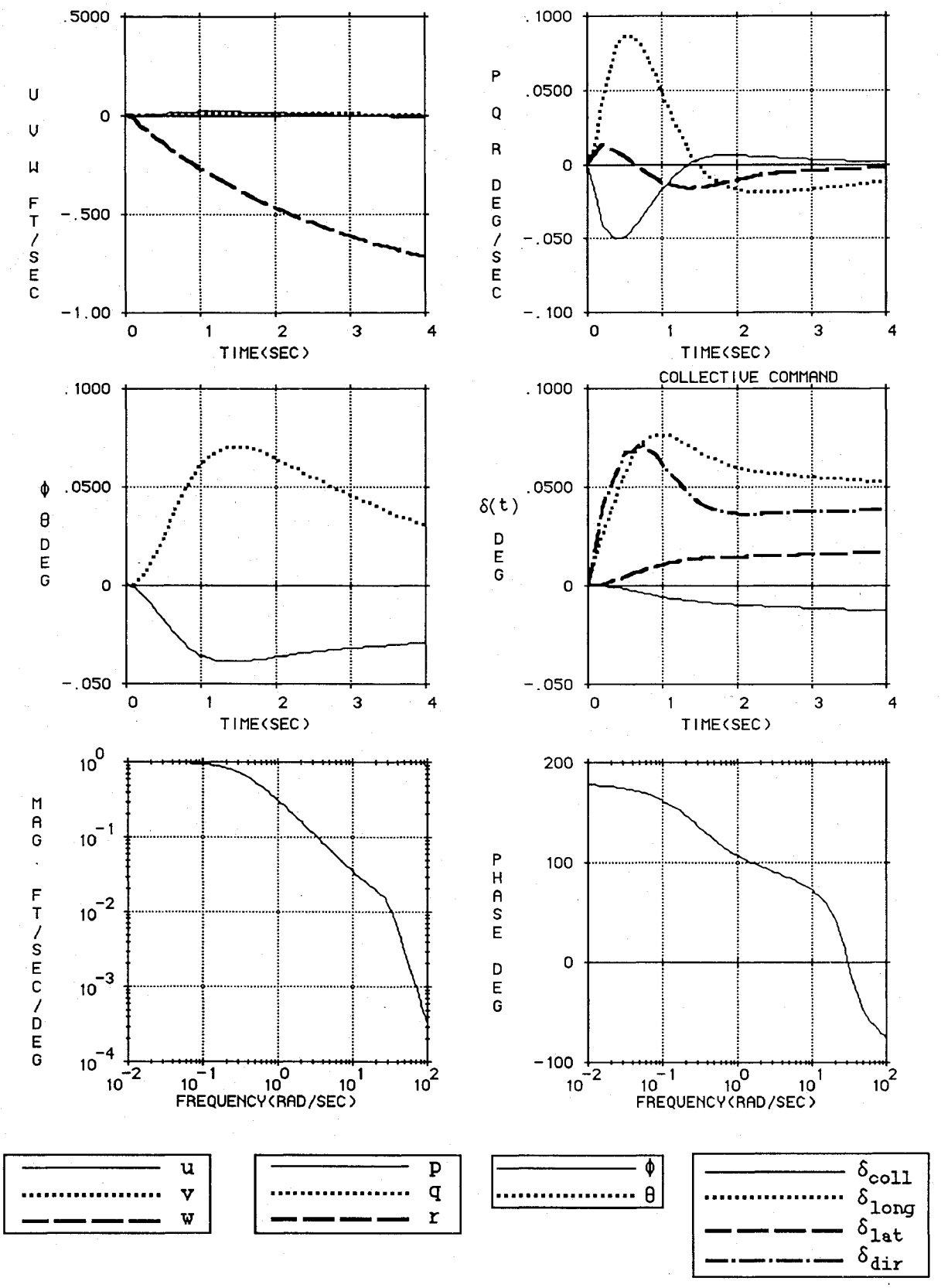

Fig. 6 Step response for a collective input, controller effort and Bode plots for $w(s)/\delta_{coll}(s)$.

As mentioned previously, due to the significant control coupling a prefilter must be implemented to convert the pilot inputs to that of controller inputs. A prefilter gain matrix P is calculated so that the input distribution matrix when postmultiplied by P forces certain states to specified values in the steady state, thus decoupling the control matrix. Since our model has four outputs, we can only specify the steady-state values for four states. Let the closed-loop equations be

$$\dot{x} = (A - BG)x + Bu \tag{13a}$$

$$y = Wx \tag{13b}$$

where y is the desired four states to be specified, and W is a matrix that selects the desired states from x. Taking the

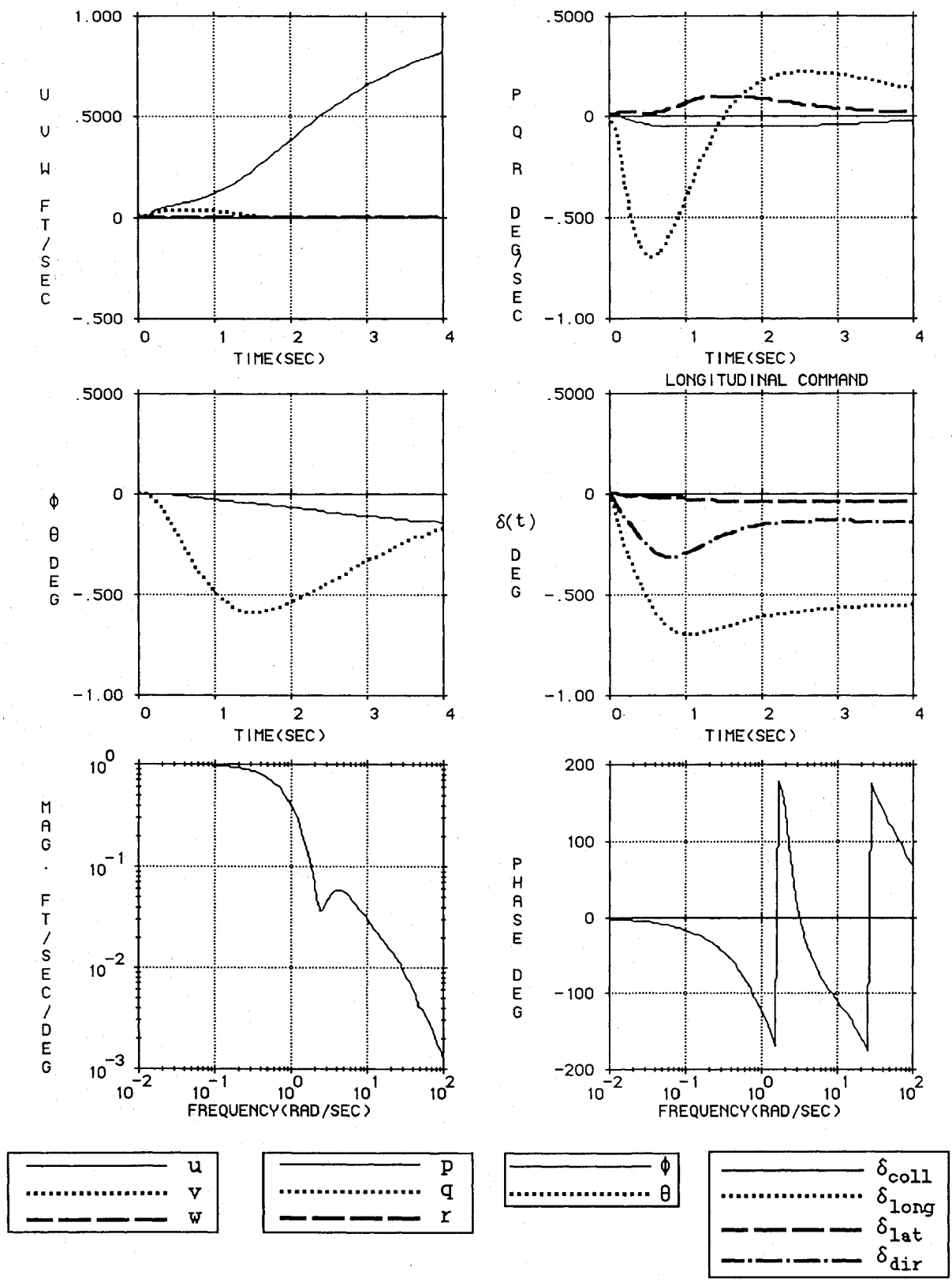

Fig. 7 Step response for a longitudinal input, controller effort and Bode plots for $u(s)/\delta_{long}(s)$.

Laplace transform of Eq. (13), we have

$$y(s) = W(sI - A + BG)^{-1}Bu(s)$$

Then for a unit step $u(t)$

$$y(s) = W(sI - A + BG)^{-1}B(u_c/s)$$

Now, applying the final value theorem, the values for the steady state y are

$$y_{ss} = \lim sy(s) = W(-A + BG)^{-1}Bu_c, \qquad s \to 0$$

Finally, solve for the u_c required to obtain specified steady-state values

$$u_c = [W(-A + BG)^{-1}B]^{-1}y$$

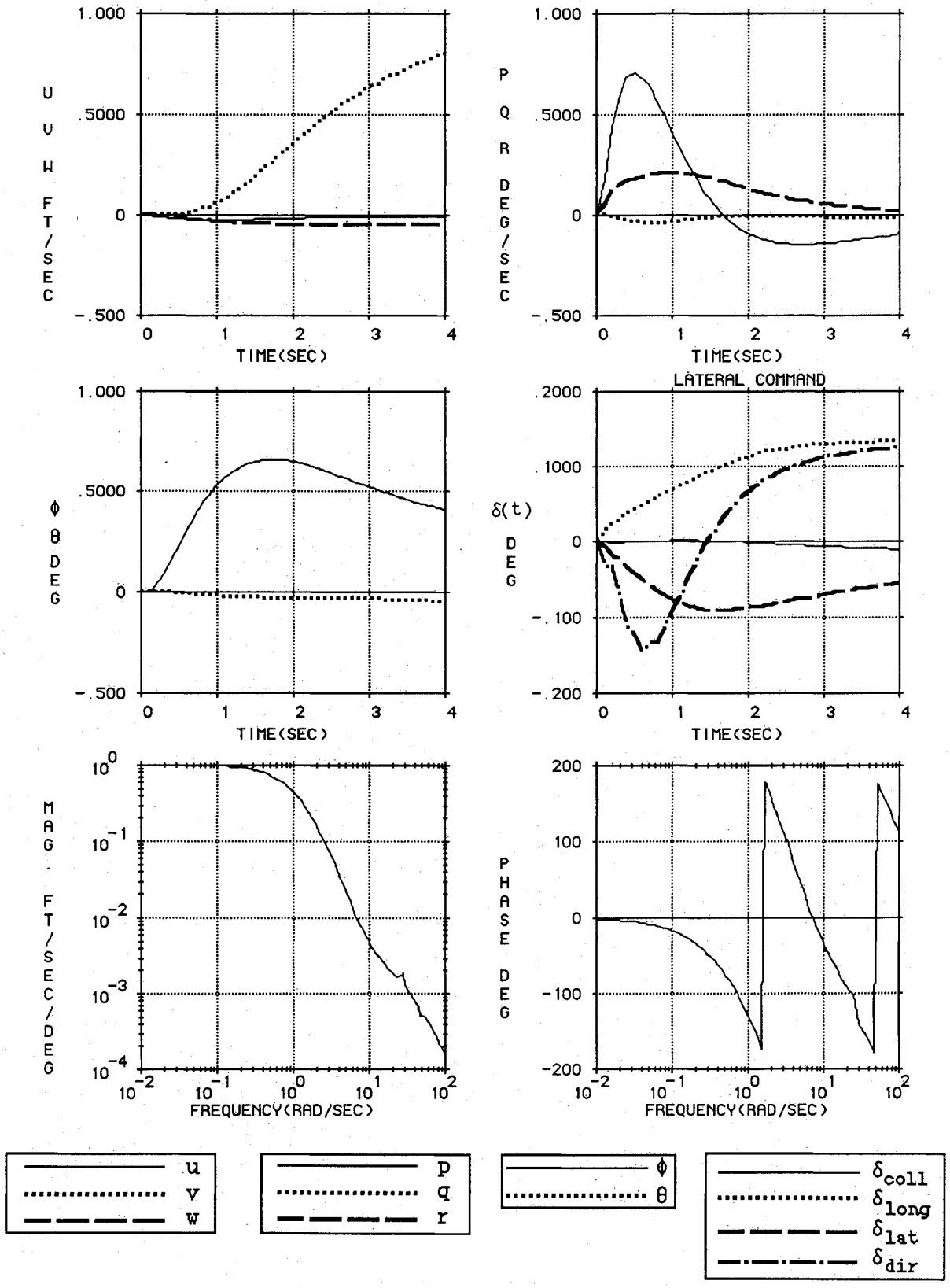

Fig. 8 Step response for a lateral input, controller effort and Bode plots for $v(s)/\delta_{lat}(s)$.

The matrix P is then given by

$$P = [u_{cw} \quad u_{cu} \quad u_{cv} \quad u_{cr}]$$

Then the closed-loop equation becomes

$$\dot{x} = (A - BG)x + BPu_p$$

where u_p is now the pilot command. This technique was applied to the 10th-order model, but when the closed-loop system was realized for the 29th-order model, yielding a 39th-order system, the decoupling was not as significant as expected. The technique was then used with the 39th-order closed-loop system, and this prefilter achieved the desired decoupling. The final prefilter gain P is given in Table 3.

Performance Evaluation

The stability of the closed-loop system using the reduced 10th-order model with regard to perturbations $\Delta(s)$ is

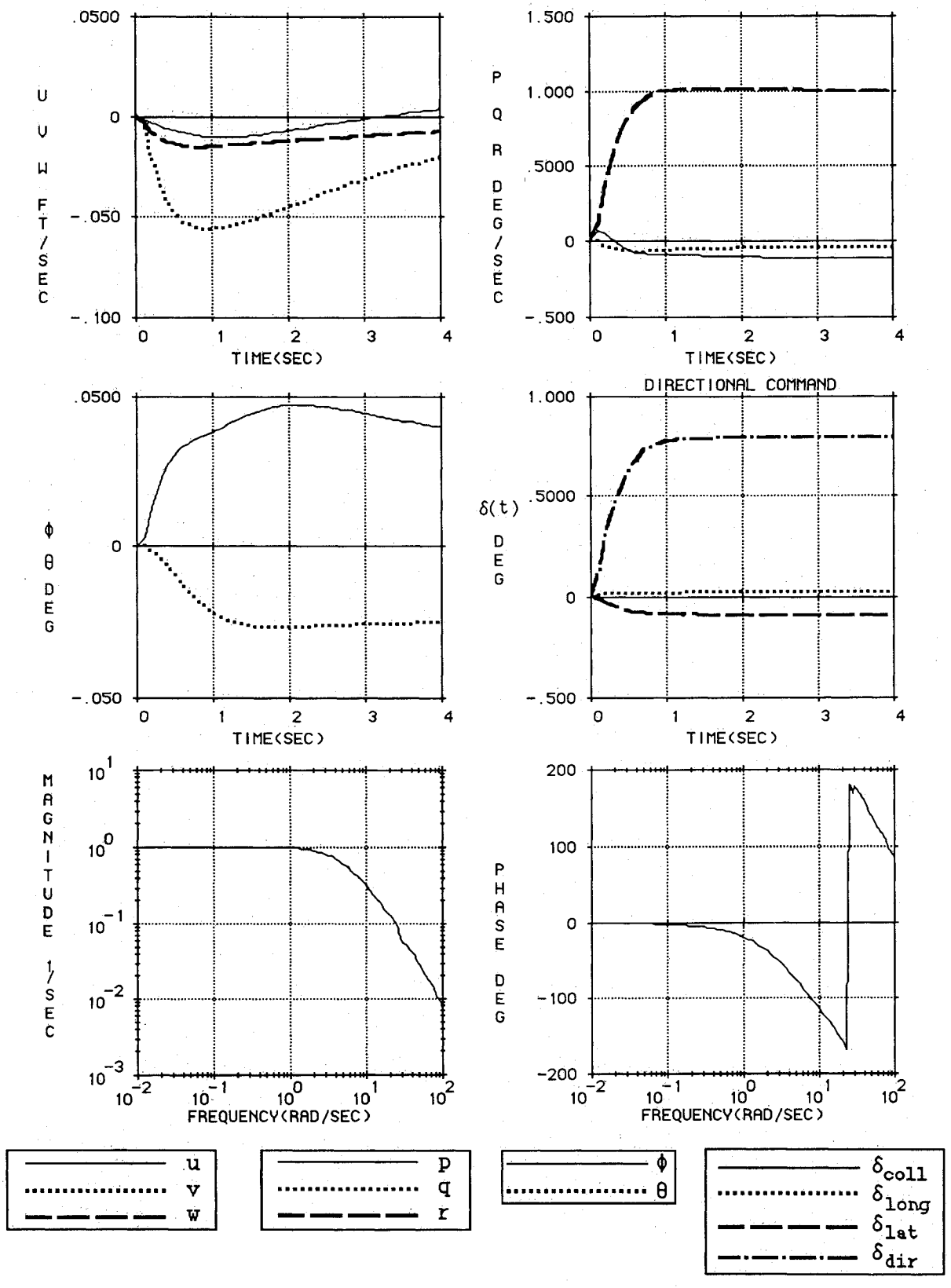

Fig. 9 Step response for a directional input, controller effort and Bode plots for $r(s)/\delta_{dir}(s)$.

evaluated by applying the stability robustness theorem.[8] If the following is true:

$$\underline{\sigma}\left(I + [K(i\omega)G_r(i\omega)]^{-1}\right) \geq \bar{\sigma}[\Delta(i\omega)]\forall\omega$$

then the reduced-order model and compensator will be robustly stable in the presence of uncertainty, i.e., unmodeled dynamics. This is just a sufficient condition and is generally conservative. This test evaluates the closed-loop stability of the perturbed system for a large class of perturbations with a single test. Figure 5 shows the stability robustness test applied to this problem. The test is not satisfied, but again this is only a sufficient condition, not a necessary one, and only indicates that the stability may be compromised when utilizing the original 29th-order system, or that the reduced-order model and compensator will not be robust with respect to uncertainties in

the plant. Since the main purpose is to design a suboptimal controller for the 29th-order system, the primary concern is the stability of $G_{29}(s)$ compensated with $K(s)$. The performance of the compensator designed with the 10th-order model is evaluated with respect to the 29th-order model. The closed-loop 39th-order system is realized as

$$\begin{bmatrix} \dot{x} \\ \dot{\hat{x}} \end{bmatrix} = \begin{bmatrix} A_{29} & -B_{29}G \\ HC_{29} & A_{10}-B_{10}G-HC_{10} \end{bmatrix} \begin{bmatrix} x \\ \hat{x} \end{bmatrix} + \begin{bmatrix} B_{29}P \\ B_{10}P \end{bmatrix} u_p \quad (14a)$$

$$y = \begin{bmatrix} C_{29} & 0 \end{bmatrix} \begin{bmatrix} x \\ \hat{x} \end{bmatrix} \quad (14b)$$

All of the closed-loop poles for system 14 are stable, but due to the small damping factors in the low-frequency poles in actual piloted simulations it is possible that due to nonlinearities in the system these eigenvalues may drift and become unstable.[2] The transient response characteristics due to a step input for the four control inputs for Eq. (14) are shown in Figs. 6–9. Velocity maneuver responses are for 1 ft/s pilot input step command. The yaw maneuver is for a 1 deg/s pilot input step command. The controller effort for each step response is shown in Figs. 6–9. Bode plots for u,v,w,r with respect to their corresponding control inputs were calculated and are also shown in Figs. 6–9. Examining the step responses for a collective input (Fig. 6), it can be seen that excellent decoupling is achieved. The bode plot for $w(s)/\delta_{coll}(s)$ exhibits the desired first-order response. Examining the step responses in Figs. 7–9, longitudinal, lateral, and directional, respectively, extremely good decoupling from the other axes is illustrated. The bode plots for $u(s)/\delta_{long}(s)$, $v(s)/\delta_{lat}(s)$, $r(s)/\delta_{dir}(s)$ exhibit, as did the transient responses, the desired properties of a decoupled system, with second-order responses in u,v and first-order response in r. If a pilot is modeled as a pure gain and closes the loop for each channel, from Figs. 6–9 (after normalizing dc gain to unity) the system would have 180-deg phase margin and infinite gain margin in heave, 160-deg phase margin and 15 dB gain margin in longitudinal, 140-deg phase margin and 12 dB gain margin in lateral, and 160-deg phase margin and 20 dB gain margin in yaw. The system with the pilot in the loop would have bandwidths of 0.34 rad/s in heave, 0.6 rad/s in longitudinal and lateral, and 4 rad/s in yaw.

Conclusion

This paper has presented the synthesis of a reduced-order model and controller design for a modern attack helicopter. Good decoupling of the control axes was achieved, contributing to pilot work load reduction. Time and frequency response characteristics were consistent with specified criteria. The controller developed serves as an excellent base point in a system design for the highly nonlinear helicopter. The technique of balanced coordinates for obtaining a reduced-order model, eigenstructure assignment, and loop-transfer recovery appear to be excellent techniques for the design of a multivariable flight control system.

Acknowledgment

This research was partially supported by the Army Research Office under Contract DAAL03-86-K-0056. The author would like to acknowledge the invaluable assistance of Dr. William Garrard of the Department of Aerospace Engineering and Mechanics at the University of Minnesota. All computing and graphics presented here were performed on *MAControl*™, a control systems software for the Apple Macintosh computer.

References

[1]Garrard, W. L., and Liebst, B. S., "Design of a Multivariable Helicopter Control System Design for Handling Qualities Enhancement," *Proceedings of the 43rd Annual American Helicopter Society Forum,* St. Louis, MO, May 1987, pp. 677–696.

[2]Enns, D., "Multivariable Flight Control for an Attack Helicopter," *Proceedings of the 1986 Automatic Control Conference,* Williamsburg, VA, June 1986.

[3]Moore, B. C., "Principal Component Analysis in Linear Systems: Controllability, Observability, and Model Reduction," *IEEE Transactions on Automatic Control,* Vol. 26, No. 1, 1981.

[4]Laub, A. J., "Computation of 'Balancing' Transformations," *Proceedings of the Joint Automatic Control Conference,* FA8-E, San Francisco, CA, 1980.

[5]Ekblad, M., "On the Compatibility of Eigenstructure Assignment and Reduced Order Modeling," M.S. Thesis, Univ. of Minnesota, Oct. 1987.

[6]Lehtomaki, N., et al., "Robustness Tests Utilizing the Structure of Modeling Error," *Proceedings of the 1981 IEEE Conference on Decision and Control,* Inst. of Electrical and Electronics Engineers, New York, Dec. 1981, pp. 1173–1190.

[7]Liebst, B. S., Garrard, W. L., and Adams, W. M., "Design of an Active Flutter Suppression System," *Journal of Guidance, Control, and Dynamics,* Vol. 8, No. 1, 1986, pp. 64–71.

[8]Moore, B. C., "On the Flexibility Offered by Full State Feedback in Multivariable Systems Beyond Closed Loop Eigenvalue Assignment," *IEEE Transactions on Automatic Control,* Vol. 21, Oct. 1976, pp. 682–691.

[9]Mitchell, D., and Hoh, R., "Development of Time Response Criteria for Rotorcraft at Hover and Low Speeds," AIAA Paper 85-1790, 12th Atmospheric Flight Mechanics Conference, Snowmass, CO, Aug. 1985.

[10]Doyle, J. C., and Stein, G., "Multivariable Feedback Design: Concepts for a Classical Modern Synthesis," *IEEE Transactions on Automatic Control,* Vol. 26, Feb. 1981, pp. 4–16.